Carbohydrate Polymers 343 (2024) 122434

Contents lists available at ScienceDirect

Carbohydrate Polymers

journal homepage: www.elsevier.com/locate/carbpol

Unraveling the unique structural motifs of glucuronoxylan from hybrid aspen wood

Pramod Sivan [a], Emilia Heinonen [a,b], Louis Escudero [a], Madhavi Latha Gandla [c], Amparo Jiménez-Quero [a], Leif J. Jönsson [c], Ewa J. Mellerowicz [d], Francisco Vilaplana [a,b,*]

[a] Division of Glycoscience, Department of Chemistry, KTH Royal Institute of Technology, AlbaNova University Centre, 106 91 Stockholm, Sweden
[b] Wallenberg Wood Science Centre (WWSC), KTH Royal Institute of Technology, 100 44 Stockholm, Sweden
[c] Department of Chemistry, Umeå University, 901 87 Umeå, Sweden
[d] Umeå Plant Science Centre, Swedish University of Agricultural Sciences, Department of Forest Genetics and Plant Physiology, 901 83 Umeå, Sweden

ARTICLE INFO

Keywords:
Hybrid aspen
Glucuronoxylan
Glycan sequencing
Acetylation

ABSTRACT

Xylan is a fundamental structural polysaccharide in plant secondary cell walls and a valuable resource for biorefinery applications. Deciphering the molecular motifs of xylans that mediate their interaction with cellulose and lignin is fundamental to understand the structural integrity of plant cell walls and to design lignocellulosic materials. In the present study, we investigated the pattern of acetylation and glucuronidation substitution in hardwood glucuronoxylan (GX) extracted from aspen wood using subcritical water and alkaline conditions. Enzymatic digestions of GX with β-xylanases from glycosyl hydrolase (GH) families GH10, GH11 and GH30 generated xylo-oligosaccharides with controlled structures amenable for mass spectrometric glycan sequencing. We identified the occurrence of intramolecular motifs in aspen GX with block repeats of even glucuronidation (every 2 xylose units) and consecutive glucuronidation, which are unique features for hardwood xylans. The acetylation pattern of aspen GX shows major domains with evenly-spaced decorations, together with minor stretches of highly acetylated domains. These heterogenous patterns of GX can be correlated with its extractability and with its potential interaction with lignin and cellulose. Our study provides new insights into the molecular structure of xylan in hardwood species, which has fundamental implications for overcoming lignocellulose recalcitrance during biochemical conversion.

1. Introduction

The carbon dioxide fixed by plants and stored as macromolecules constituting the secondary cell wall in woody tissues represents the most abundant renewable biological resource available for production of sustainable materials, chemicals and energy. Lignocellulosic biomass consists of a complex network of cellulose microfibrils embedded within the compactly intertwined matrix of hemicellulose and lignin (Martínez-Abad, Giummarella, Lawoko and Vilaplana, 2018). The major hemicellulose components of secondary cell walls of vascular plants are xylan and glucomannan (McKee et al., 2016; Willför et al., 2005). Acetylated glucuronoxylan constitutes the main hemicellulose component in hardwoods, which can account for up to 30 % dry weight of the xylem (Smith et al., 2017). The general molecular structure of hardwood xylans consists of a backbone of β-(1 → 4) D-xylopyranose units (Xyl*p*), with 4-*O*-methyl-D-glucuronic acid (mGlcA) substitutions at the *O*-2 position by an α-(1 → 2) linkage and chemically modified by acetylation at positions *O*-2, *O*-3, and *O*-2,3 in the xylose units depending on the plant type, tissue, and developmental stage (Busse-Wicher, Li, et al., 2016; Martínez-Abad et al., 2017). In hardwoods, the GX populations have different domains with distinct substitution patterns, including a major domain with even mGlcA spacing and acetylation and a highly recalcitrant domain characterized by tighter glucuronidation spacing and reduction in acetylation (Bromley et al., 2013; Busse-Wicher et al., 2014; Chong et al., 2014). Softwood arabinoglucuronoxylans (AGX) have a distinct structure compared to their hardwood counterparts, with a backbone of β-(1 → 4) D-Xyl*p* units decorated by α-(1 → 2) mGlcA and α-(1 → 3) L-arabinofuranose (Araf) and no acetylation. The intramolecular substitution pattern is well conserved, with a major domain with an even pattern of mGlcA substitutions every 6 Xyl*p* units and Ara*f*

* Corresponding author at: Division of Glycoscience, Department of Chemistry, KTH Royal Institute of Technology, AlbaNova University Centre, 106 91 Stockholm, Sweden.
E-mail address: franvila@kth.se (F. Vilaplana).

https://doi.org/10.1016/j.carbpol.2024.122434
Received 7 May 2024; Received in revised form 11 June 2024; Accepted 24 June 2024
Available online 25 June 2024

decorations evenly spaced from these anchoring mGlcA units, and a minor domain with well-conserved consecutive spacing of mGlcA units (Martínez-Abad et al., 2017). These substitutions are necessary to maintain xylan solubility (Mikkelsen et al., 2015) while unsubstituted xylan forms crystalline fibres of chains adopting a 2-fold or 3-fold screw helix depending on the environment (Nieduszynski & Marchessault, 1971).

The genetic diversity, adaptability, and biological function of plants have been modulated by evolving biosynthetic processes and resulted in plant cell wall polysaccharides that are heterogeneous in composition and molecular structure (Burton et al., 2010). Deciphering molecular structures of xylans from different softwood and angiosperm species helps to understand the complex evolutionary biology of matrix polysaccharides and its relationship with wood properties such as biomass recalcitrance. In this regard, the xylan substitution pattern in four different gymnosperm lineages (Conifers, Cycads, Ginkgo, and Gnetophyta) revealed that the mGlcA substitution of xylan is similar in the four lineages, with repeating mGlcA units on every sixth xylosyl residue and Ara*f* units spaced two xylosyl residues away from those containing mGlcA (Busse-Wicher, Li, et al., 2016). However, subtle differences have been noticed among different plant groups such as a relatively higher arabinosylation in Ginkgo and Cycads compared to conifers, the absence of arabinose substitution and the presence of acetyl decorations in Gnetophyta (similar to secondary cell wall xylan in eudicots). These variations among different plant groups suggest that molecular diversity in xylan decorations might have evolved among different evolutionary groups in order to adapt to the composition of the specific cell walls and to tune the microfibril interactions between different lignin (G type in conifers and GS type in eudicots) and hemicellulose cell wall components.

The molecular structure of hemicelluloses is believed to modulate their interactions with cellulose microfibrils (Bromley et al., 2013; Busse-Wicher et al., 2014; Busse-Wicher, Li, et al., 2016; Martínez-Abad et al., 2017; Martínez-Abad, Jiménez-Quero, & Wohlert, 2020) and the occurrence of covalent linkages with lignins (Giummarella et al., 2019; Lawoko et al., 2005). The acetyl decorations are suggested to contribute to an hydrophobic environment across the xylan backbone, whereas the glucuronic acid groups may provide acidic microenvironments (Simmons et al., 2016). The xylan macromolecule is proposed to have two conformations, a two-fold helical screw domain with acetyl and mGlcA decorations facing the same directions (even spacing) and threefold screw domain with tight mGlcA spacing without any preference for even spacing (Bromley et al., 2013; Busse-Wicher et al., 2014). Therefore, on a xylan backbone in the ribbon-like 2-fold helical screw conformation, all the decorations will face one side and this allow unsubstituted face of xylan for hydrogen bonding to the hydrophilic surface of cellulose-forming xylanocellulose fibrils (Busse-Wicher et al., 2014; Busse-Wicher, Li, et al., 2016; Simmons et al., 2016). The NMR analysis of GX populations from birch wood (Martínez-Abad, Giummarella, Lawoko and Vilaplana, 2018) revealed that easily extractable GX interacts with lignin by γ-ester linkages (between mGlcA and the γ-carbon of lignin) while the recalcitrant GX populations shows more benzyl ether linkages.

The choice of extraction method has a significant impact on the molecular structure and the extent of degradation of the polysaccharides. Unlike common alkali-based methods, subcritical water extraction (SWE) preserves the labile, native chemical functionalities such as acetylations and feruloylations (Martínez-Abad, Giummarella, Lawoko, Vilaplana, 2018). Our recent work demonstrated the potential of SWE as pretreatment in biorefinery processes, enhancing the saccharification efficiency of aspen wood by solubilizing hemicellulose and reducing wood recalcitrance (Sivan et al., 2023). However, the specific molecular characteristics of aspen GX and their influence on lignocellulose recalcitrance remain largely unknown. Here, we investigated the molecular structure of GX extracted from hybrid aspen using comprehensive mass-spectrometry-based glycan sequencing. Our results revealed unique structural motifs in the aspen GX in terms of acetyl and glucuronyl substitution pattern, which provides more insight into the interaction of GX with cellulose and lignin.

2. Experimental

2.1. Plant material

Wood was harvested from field grown hybrid aspen (*Populus tremula* L. x *tremuloides* Michx.) clone T89 planted in June 2011 at flat and homogeneous area in Växtorp, Laholm community, Sweden (56.42°N, 13.07°E), where they were grown for five seasons (Donev et al., 2023). The wood was ground to a rough powder in a Cutting Mill SM 300 using 2 mm sieve (Retsch, Haan, Germany). Rough powder was then sieved on a vibratory sieve shaker AS 200 (Retsch) to obtain the 100–500 μm particle size fraction.

2.2. Hemicellulose extraction

2.2.1. Subcritical water extraction

Four wood powder samples (2 g) representing material from pool of 32 trees were extracted in 0.2 M sodium formate buffer (pH 5.0), at 170 °C and 100 bar pressure with an accelerated solvent extractor (ASE-300, Dionex, USA). Extraction proceeded in four consecutive steps with residence times of 10, 20, 30 and 60 min. The extraction conditions (temperature, pH and duration) were implemented following previously optimized conditions for hardwoods and softwoods (Martínez-Abad, Giummarella, Lawoko, Vilaplana, 2018; Martínez-Abad, Jiménez-Quero, & Wohlert, 2020). Salts and low molecular weight compounds were removed by dialysis using Spectra/Por 3 membranes (Spectrum, USA), after which the extracted polymers were freeze-dried and stored at −20 °C prior to analysis.

2.2.2. Alkaline extraction

The alkaline extraction of the hemicelluloses from the aspen wood powder was performed using 1 g of powder by incubating it with 15 mL of 24 % KOH for 24 h at room temperature (Escalante et al., 2012; Timell, 1961). The extract was filtered through 60 μm wire and neutralized with 0.4 volumes of acetic acid. The hemicelluloses were precipitated overnight with four volumes of 96 % ethanol at 4 °C, the precipitate was centrifuged, washed in 80 % ethanol, dissolved in distilled water and freeze dried prior to analysis.

2.3. Chemical characterization of hemicellulose extracts

2.3.1. Pyrolysis gas chromatography combined with mass spectrometry (Py-GC/MS)

Py-GC/MS was performed on subcritical water extracts and freeze-dried alkaline extracts, as previously described (Gandla et al., 2015). Fifty μg (± 10 μg) of powder was applied to a pyrolyzer equipped with an autosampler (PY-2020iD and AS-1020E, Frontier Lab, Japan) connected to a GC/MS (7890 A/5975C; Agilent Technologies AB, Sweden). The pyrolysate was separated and analyzed as previously described (Gerber, Eliasson, Trygg, Moritz, & Sundberg, 2012).

2.3.2. Size exclusion chromatography

Molar mass of the extracted polymers was determined by size exclusion chromatography coupled to refractive index and UV-detectors (SECurity 1260, Polymer Standard Services, Mainz, Germany). The samples were dissolved at a concentration of 2 mg/mL in dimethyl sulfoxide (DMSO Anhydrous, Sigma-Aldrich) with 0.5 % *w*/w LiBr (Anhydrous free-flowing Redi-Dri, Sigma-Aldrich, USA) at 60 °C, and filtered through 0.45 μm PTFE syringe filters (VWR). The separation was carried through GRAM Analytical columns of 100 and 10,000 Å (Polymer Standard Services, Mainz, Germany) at a flow rate of 0.5 mL/min and 60 °C using the same eluent as for dissolving the samples. The columns were calibrated using pullulan standards between 345 and

708,000 Da (Polymer Standard Services, Germany).

2.3.3. Acetyl content by liquid chromatography

The acetyl content was determined in duplicates by saponification and subsequent determination of the released acetic acid by HPLC-UV. Shortly, 5 mg of sample was incubated overnight in 0.8 M NaOH at 60 °C with constant mixing. Samples were then neutralized with 37 % HCl and filtered through 0.2 μm Chromacol syringe filters (17-SF-02(N), Thermo Fisher Scientific, USA). The acetic acid was detected by UV at 210 nm (HPLC-UV Dionex-Thermofisher Ultimate 3100, USA), after separation with a Rezex ROA-organic acid column (300 × 7.8 mm, Phenomenex, USA) at 50 °C in a 2.5 mM H_2SO_4 at 0.5 mL/min. Propionic acid was used as an internal standard. The degree of xylan acetylation was calculated as the ratio of Xyl*p* bearing acetylation from using the total acetyl and xylose content, as previously reported (Bi et al., 2016).

2.4. Enzymatic hydrolysis

For enzymatic depolymerization, the xylan fractions from alkaline extraction and 30 min extracts of SWE process were digested using GH10 *endo*-β-(1 → 4)-xylanase from *Cellvibrio mixtus* (Megazyme, Ireland), a GH11 endo-β-(1 → 4)-xylanase from *Neocallimastix patriciarum* (Megazyme, Ireland) and GH30 endo β-(1 → 4) glucuronoxylanase (kindly provided by Prof. James F. Preston, University of Florida). Enzymatic hydrolysis was performed by incubating 1 mg of each extract in 250 μL of 20 mM sodium acetate buffer (pH 5.5,) with enzyme (10 U mL^{-1}) for 16 h at 37 °C. After incubation, the enzyme was inactivated at 95 °C and the mixture was filtered.

2.5. Oligosaccharide mass profiling (OLIMP)

The oligosaccharide profiles after enzymatic digestion were analyzed by high-performance anion-exchange chromatography with pulsed amperometric detection (HPAEC-PAD) as previously reported (McKee et al., 2016). Linear xylo-oligosaccharides (X2-X6; Megazyme, Ireland) were used as external standards. Oligomeric mass profiling (OLIMP) was performed by electrospray ionization mass spectrometry (ESI-MS) using a Synapt HDMS mass spectrometer in positive mode (Waters, USA). Enzymatic hydrolysates were diluted to 0.1 mg/mL concentration using acetonitrile 50 % (*v*/v) with 0.1 % (v/v) formic acid and filtered through Chromacol 0.2 μm filters (Scantec Nordic, Sweden). Samples were then briefly passed through a ZORBAX Eclipse Plus C18 column 1.8 μm (2.1 × 50 mm) (Agilent Technologies, Santa Clara, CA, USA) for automation and analyzed using positive-ion mode in the ESI-MS. The capillary and cone voltage were set to 3 kV and 70 V, respectively. The oligosaccharides were detected as $[M + Na]^+$ adducts.

2.6. Oligosaccharide separation and sequencing by tandem LC-MS/MS

Oligosaccharide sequencing was achieved after separation of labelled oligosaccharides by LC-ESI-MS/MS. Derivatization was performed by reductive amination with anthranilic acid, as previously described (Mischnick, 2012). The labelled oligosaccharides were separated through an ACQUITY UPLC HSS T3 column (150 × 2.1 mm, Waters, USA) at a flow rate of 0.3 mL/min and a gradient of increasing acetonitrile content (10–30 %) over 40 min. Mass spectrometric (MS) analysis was performed in positive mode with the capillary voltage and cone set to 3 V and 70 V, respectively. MS^2 was performed by selecting the *m/z* of interest through single ion monitoring (SIM) and subjecting it to collision-induced dissociation (CID) using argon as collision gas, at a ramped voltage of 35–85 V. Assignation of the proposed structures was performed by reference to labelled standards and analysis of the fragmentation spectra using ChemDraw (PerkinElmer, Waltham, Massachusetts, USA).

2.7. Nuclear Magnetic Resonance (NMR) analysis

Samples were dissolved in D_20 at 5 mg/mL and DSS-d_6 (Deuterated 3-(trimethylsilyl)-1-propanesulfonic acid sodium salt) was used as an internal reference. Heteronuclear single-quantum-coherence (HSQC) experiments (pulse sequence hsqcetgpsi) were recorded on a Bruker 400 DMX instrument (Bruker Corp., Billerica, MA, USA) with a multinuclear inverse *Z*-grad probe. The pulse length was set to 8.0 s and the relaxation delay to 2.5 s. The number of scans was 112. The spectra were phased with TopSpin (Bruker Corp., Billerica, MA, USA) and further processing was done using MestreNova (Mestrelab Research, S.L. Spain).

3. Results and discussion

Hybrid aspen is a model tree species for the study of hardwood structure and chemistry. Furthermore, aspen wood constitutes a promising biorefinery feedstock due to its fast growth and desirable structural and chemical features. In our previous work, a hemicellulose-first extraction approach using subcritical water extraction enhanced saccharification efficiency without acid pre-treatment in aspen wood (Sivan et al., 2023). Therefore, unraveling the structural features of aspen hemicelluloses and particularly GX is a key to understand their molecular interactions with cellulose and lignin that regulate biomass recalcitrance in aspen wood. Our study aims to reveal the structural motifs along the polymer backbone, the glucuronidation pattern and acetylation pattern, using xylanolytic enzymatic cleavage and liquid chromatography mass spectrometry methods.

3.1. Alkaline and subcritical water extractions provide distinct GX populations from aspen wood

The conditions of the extraction processes for the solubilization of hemicelluloses from lignocellulosic biomass have a large effect on their molecular structure. Acetyl substitutions are easily removed during alkaline extraction, whereas SWE under buffered conditions and shorter extraction times is able to prevent autohydrolysis and preserve the acetyl groups (Fig. 1A). In the present study, we used both alkaline and subcritical extraction to decipher the acetylation pattern and glucuronidation pattern in the easily extractable and recalcitrant xylan motifs from aspen (Fig. 1A). Interestingly, the subcritical water extract (SWE) showed higher xylan content compared to the alkaline extract (AE), albeit no significant differences were found in the mGlcA/Xyl ratios (an average of one mGlcA every 4–5 xylose units) (Table 1). The acetyl content analysis of SWE revealed that the degree of xylan acetylation is in a range of 0.2–0.25 which corresponds to an average of 1–2 acetyl groups per 2–3 xylose units. On the other hand, acetyl content was not detected in alkaline extract due to deacetylation of the xylan under harsh alkaline conditions. Pyrolysis-GC/MS confirmed the occurrence of higher lignin and phenolic contents in the alkaline extracts compared to SWE (Table 1). The lignin subunit composition showed much higher guaiacyl (G) lignin content and much lower syringyl:guaiacyl (S/G) ratio in AE, suggesting more recalcitrant lignin is extracted during this process compared to SWE enriched with S units. Due to the more branched nature of G-lignin, it can act as a physical barrier contributing to biomass recalcitrance (Santos et al., 2012; Yu et al., 2014). Finally, the molar mass distribution analyzed by size exclusion chromatography revealed higher molecular weights for alkaline extraction (AE) compared to the subcritical water extract, indicating the occurrence of backbone hydrolytic degradation (Fig. 1C).

3.2. Oligomeric mass profiling reveals a large diversity of acetylation and glucuronidation patterns in aspen GX

Detailed investigation of the substitution pattern in alkaline and subcritical water extracted GXs was performed using xylanolytic enzymes with known substrate recognition towards the glucuronyl

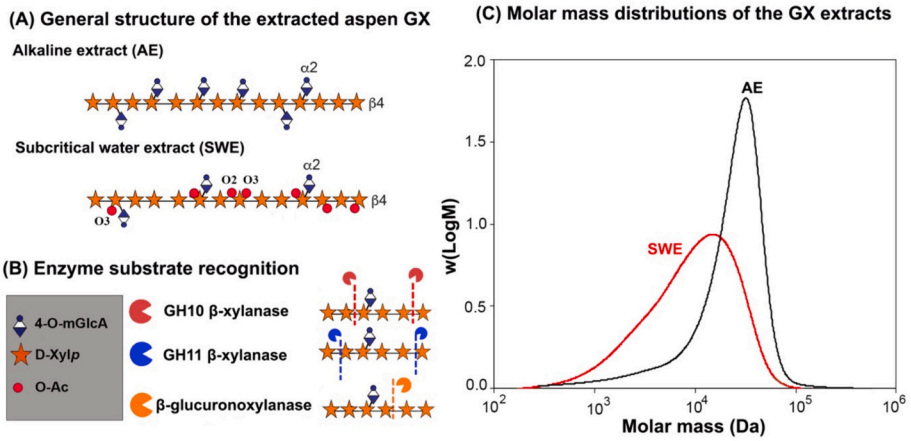

Fig. 1. (A) General structure of alkaline extract (AE) and subcritical water extract (SWE) of hardwood GX. (B) Substrate recognition pattern of xylanolytic enzyme used for GX digestion, based on previous literature (Martínez-Abad et al., 2017; Pollet et al., 2010; St John et al., 2011), (C) Molar mass distribution of aspen GX extracted using AE and SWE method.

Table 1
Chemical composition, acetylation, and molar mass distribution in alkaline extract (AE) and subcritical water extract (SWE) from aspen.

	SWE	AE
Extraction yield (wt%)[a]	8.1	7.8
Xylan yield (wt%)[b]	32.2	27.0
Carbohydrate content (mg g^{-1})[c]	838.3	993.4
Xylan content (mg g^{-1})[c]	755.4	866.6
mGlcA:Xyl ratio[c]	0.21 ± 0.01	0.17 ± 0.00
Acetyl content (%)[d]	6.8 ± 0.9	N·D
Degree of xylan acetylation[d]	0.23 ± 0.03	N·D
M_n (kDa)[e]	4.6 ± 0.0	19.6 ± 0.8
M_w (kDa)	13.3 ± 0.1	28.3 ± 0.2
Phenolic (%)[f]	0.1 ± 0.01	0.65 ± 0.09
Lignin content (%)[f]	14.5 ± 0.63	15.9 ± 0.56
Guaiacyl (%)[f]	1.8 ± 0.03	6.2 ± 0.19
Syringyl (%)[f]	10.7 ± 0.65	5.6 ± 0.40
p-Hydroxyphenyl (%)[f]	1.9 ± 0.06	3.4 ± 0.09
S/G [f]	5.8 ± 0.32	0.9 ± 0.04
C/L [f]	5.7 ± 0.28	4.9 ± 0.20

NOTE: S/G Syringyl-Guaiacyl ratio; C/L Carbohydrate-Lignin ratio; ND Not detected.

[a] Determined gravimetrically from the starting wood material.

[b] Determined based on the xylan content in the starting material (Supplementary Material Table S1).

[c] Determined from monosaccharide composition (Supplementary Material Table S1).

[d] Determined after saponification and HPLC-UV analysis.

[e] Determined by SEC-DRI.

[f] Determined from Pyrolysis GC–MS;

substitutions (Fig. 1B). GH10 and GH11 *endo* β-(1→4)-xylanases show both preference for unsubstituted xylan backbone as they are hindered by the presence of glucosyl substitution; however, GH10 xylanases require two unsubstituted Xyl*p* units for hydrolysis and can tolerate the presence of a mGlcA in the +1 position, whereas GH11 xylanases require three unsubstituted Xyl*p* units for hydrolysis and can only tolerate the presence of a mGlcA in the +2 position. This means that GH10 releases xylobiose and xylotriose with mGlcA in the non-reducing end as the main hydrolytic products, whereas GH11 xylanases produce xylotriose and a xylotetraose oligosaccharide with mGlcA bound to the second xylose unit from the non-reducing end as main products (Martínez-Abad et al., 2017; Pell et al., 2004; Pollet et al., 2010). As expected, HPAEC-PAD analysis revealed that enzymatic incubations of AE and SWE xylans with GH10 and GH11 β-xylanase digestion produced larger abundance of linear oligomers (Fig. 2A). Interestingly, both GH10 and GH11 xylanases released mainly xylotriose, which is unexpected for a GH10 xylanase. Previous kinetic studies of the hydrolysis of glucuronoxylan by a GH10 xylanase from *Cellvibrio japonicus* (*Cj*Xyn10A) at different time intervals showed a significant release of xylotriose at initial times (10–60 min), whereas longer times were required for the final conversion into xylobiose (Charnock et al., 1999; Pell et al., 2004). This suggests the incomplete digestion of aspen GX with GH10 after 24 h of incubation. As expected, the oligomeric mass profile (OLIMP) by ESI-MS from GH10 digested AE samples showed high intensity of X_3mU motifs while GH11 xylanase produced more X_4mU motifs (Fig. 2B and C). These results are in agreement with expected glucuronilated xylo-oligomers released by GH10 and GH11 xylanase enzymes (Fig. 1A) based on the available literature (Pollet et al., 2010). The prevalence of glucuronilated X_3mU and X_4mU oligosaccharides from GH10 and GH11 incubations, respectively, was observed as well for the SW xylan extracts together with the presence of different acetylated oligosaccharides (Fig. 2E and F). Interestingly, the released acetylated oligosaccharides by GH10 and GH11 incubations were different (X_3Ac for GH10 and X_4Ac for GH11), which suggest a similar tolerance for acetylations as for glucuronation.

On the contrary, GH30 β-glucuronoxylanases require the presence of a mGlcA for hydrolytic action, cleaving the glycosidic bond in the backbone one Xyl*p* unit away from the mGlcA decoration towards the reducing end (Hurlbert & Preston, 2001; St John et al., 2011; Urbániková et al., 2011). Based on this, GH30 β-glucuronoxylanases are efficient enzymes for the identification of glucuronic acid spacing in complex GX (Martínez-Abad, Giummarella, Lawoko, Vilaplana, 2018). As expected, incubation of alkaline-extracted aspen GX with β-glucuronoxylanase (GH30) released mainly glucuronilated oligomers (Fig. 2A). Interestingly, relatively higher intensity of linear oligos (without mGlcA) was observed in the oligosaccharide profiles by HPAEC-PAD produced by GH30 digested acetylated GX (Fig. 2D). As the high pH conditions during HPAEC-PAD cleave the acetyl substitutions, we can infer that the occurrence of such linear oligosaccharides arise from natively acetylated oligosaccharides, suggesting that GH30 glucuronoxylanases can also recognize acetyl groups and cleave xylan in the absence of mGlcA, as it has been previously suggested for *Arabidopsis* and birch (Busse-Wicher et al., 2014; Martínez-Abad, Giummarella, Lawoko, Vilaplana, 2018).

The pattern of mGlcA decorations in aspen GX was monitored using oligomeric mass profiling (OLIMP) by electrospray mass spectroscopy (ESI-MS/MS). The OLIMP profile from alkaline-extracted aspen digested with β-glucuronoxylanase (GH30) showed high intensity of X5mU motifs as the predominant mGlcA spacing pattern in aspen GX (Fig. 2B,C), in agreement with the mGlcA:Xyl ratio (Table 1). Similar average spacing pattern has been reported previously for GX from birch wood

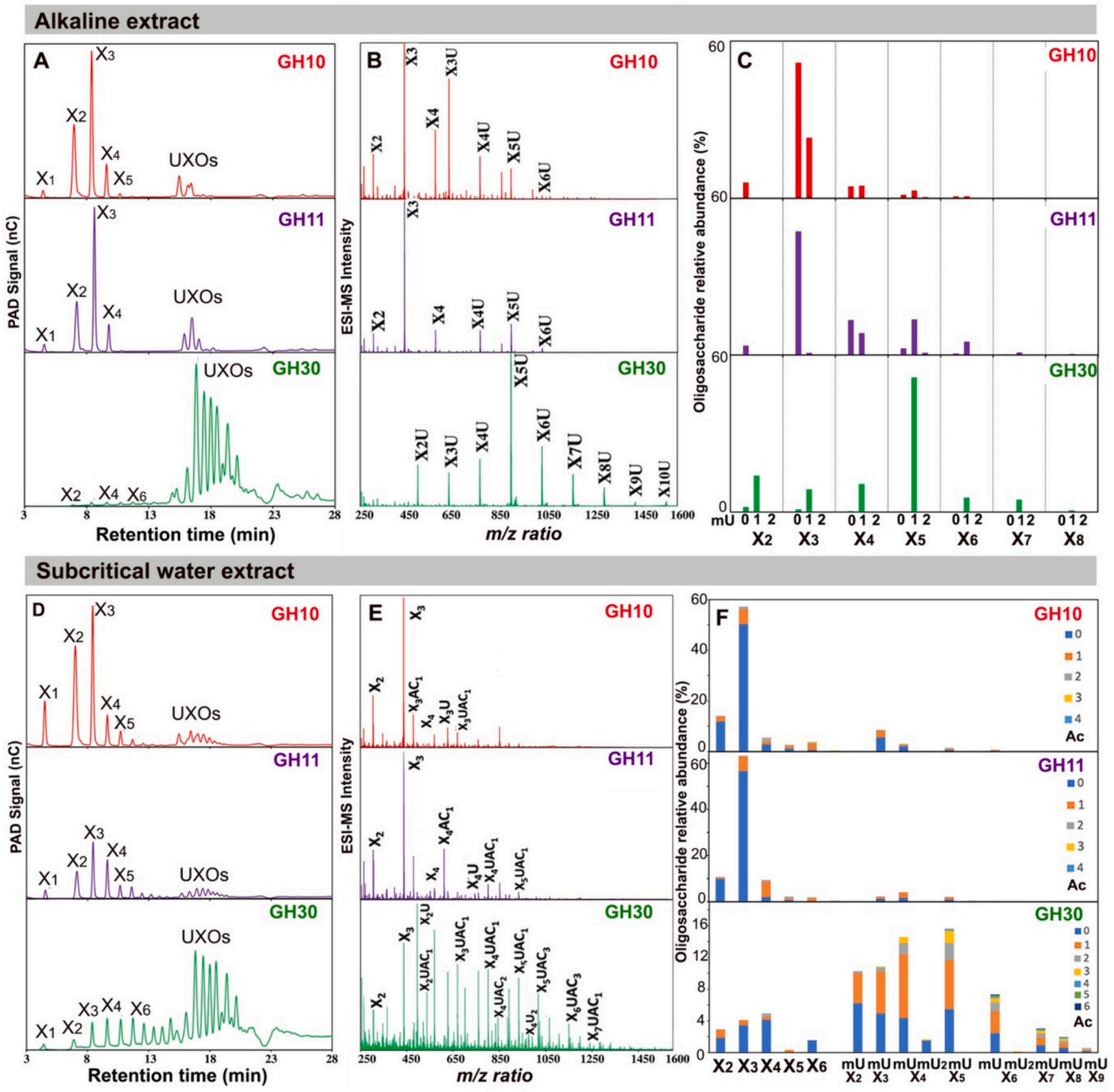

Fig. 2. Oligosaccharide profiling of aspen GX. (A,D) Oligosaccharide fingerprinting with high-performance anion-exchange chromatography with pulsed amperometric detection (HPAEC-PAD); (B,E). Oligomeric mass profiling with ESI-MS. Oligosaccharide assignment is provided in the Supplementary Material Table S2. (C,F). Relative abundance of the different oligosaccharides, calculated from the total ESI-MS intensities from triplicate digestions. NOTE: X (Xylose), Ac (Acetyl), mU (mGlcA).

(Martínez-Abad, Giummarella, Lawoko, Vilaplana, 2018). When considering GX extracted via subcritical water, the OLIMP profile from GH30 digestions shows a broad profile of acetylated UXOs, with mainly single-acetylated X_4mUAc and X_5mUAc (Fig. 2E,F) representing the even and odd spaced substitution patterns. The relative abundance of such UXOs decreases with extraction time and instead a higher abundance of shorter X_3mU populations appear in such recalcitrant GX populations (Fig. S1), which might represent a minor domain with odd and tighter glucuronidation (Martínez-Abad, Jiménez-Quero, & Wohlert, 2020). Interestingly, acetylated GX from aspen showed a relatively high intensity of X_2mU and X2mUAc compared to other angiosperms (i.e. birch, *Arabidopsis*), together with a small population with double glucuronation (X_4mU_2) that has not been reported before. The occurrence and structure of these specific motifs will be expanded in the following sections.

3.3. *Aspen GX contains blockwise patterns of X2U motifs*

We identified the occurrence of X_2mU and X_2mUAc in the acetylated GX aspen populations released by GH30 treatment. The single-ion monitoring and sequencing of such motifs by LC-MS/MS confirmed the presence of only one isomeric oligosaccharide structure for each

mass-to-charge ratio, with the mGlcA group in the non-reducing end and the acetylation in the same Xyl*p* unit bearing the mGlcA decorations (Fig. S2). This is in agreement with the cleavage pattern of GH30 β-glucuronoxylanases and the higher stability reported for the acetylations present in the Xylp units containing mGlcA (Martínez-Abad, Giummarella, Lawoko, Vilaplana, 2018).

The higher abundance of X_2U motifs in aspen GX after GH30 hydrolysis compared to other hardwood species raised an important question, this is, whether these motifs are placed randomly across the polymer backbone or whether they exist blockwise in stretches across the backbone. This might have important implications on the architecture of the aspen cell wall, as the presence of such block even motifs might promote interactions with cellulose surfaces (Simmons et al., 2016) and provide acidic microenvironments by the mGlcA decorations. To address this question, we carried out consecutive digestions of both acetylated (SWE) and deacetylated (AE) GX with GH10/GH11 followed by GH30. As GH10 and GH11 require two consecutives unsubstituted Xyl*p* units, block X_2U motifs should not be cleaved by these enzymes. On the other hand, GH30 can recognize and cleave these motifs as it needs only one unsubstituted Xyl*p* unit at the reducing end. As expected, the first digestion with GH10/GH11 did not produce X_2U oligomers while the second digestion with GH30 released X_2U motifs from the fraction undigested by GH10 and GH11 enzymes confirming the occurrence of close glucuronidation pattern as long repeats of X_2U motifs in aspen GX (Fig. 3). Since GH10 enzymes release mainly X_3U oligomers as decorated xylan oligomers, the subsequent digestion with GH30 could plausibly cleave these X_3U motifs and release X_2U and xylose (X_1). To confirm that the observed X2U motifs after double digestion with GH10/GH11 and GH30 are not coming from X_3U motifs, we evaluated the relative intensity difference in X_3U after double digestion. However, we did not notice any significant difference in X_1 and X_3U motifs between single and double digestion confirming the observed X_2U motifs are produced

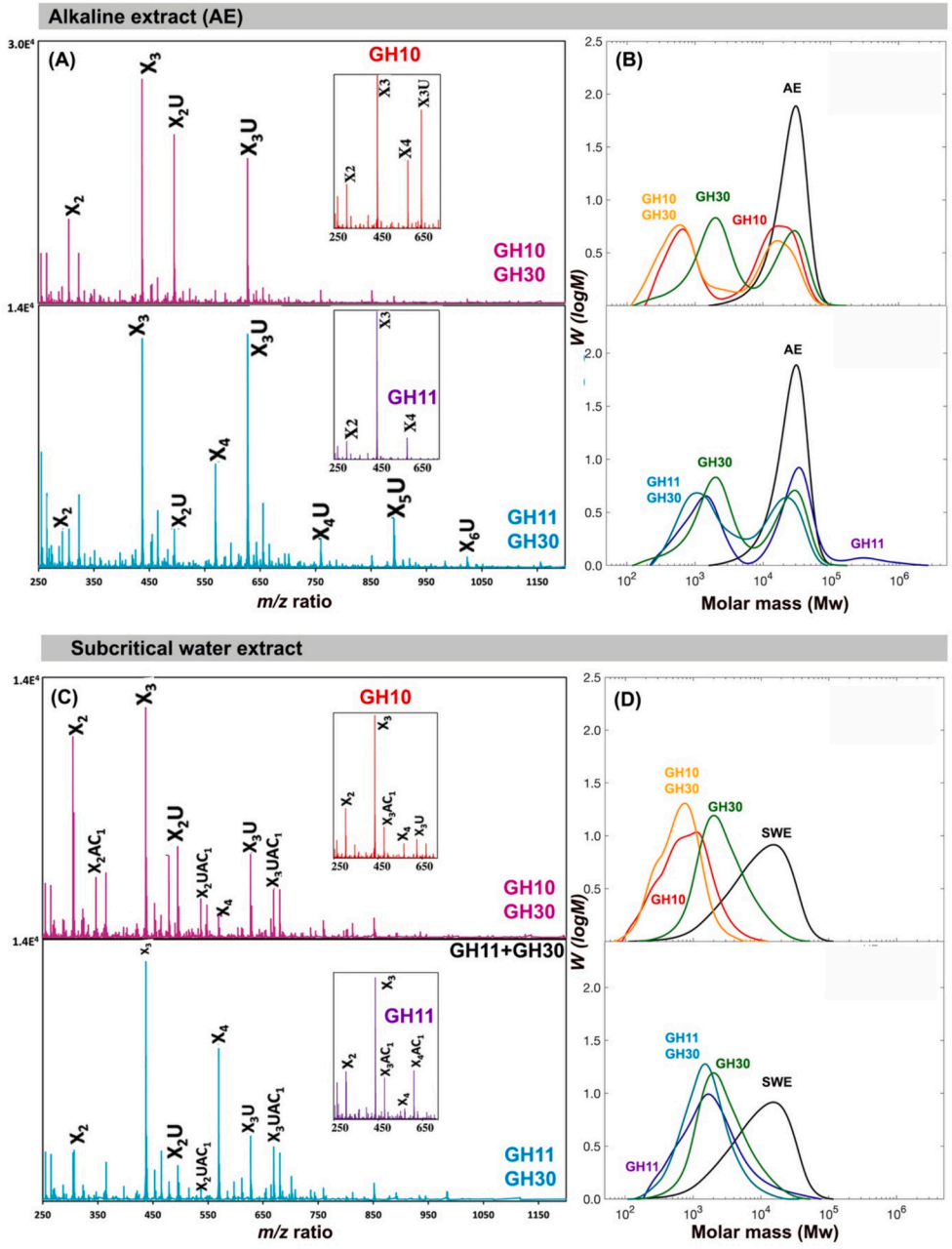

Fig. 3. Double enzymatic digestions of aspen GX with GH30 β-glucuronoxylanase and GH10 or GH11 β-xylanase. Electron-spray ionization mass spectrometry (ESI-MS) profile of (A) alkaline and (C) subcritical water extracts. Molar mass distributions of (B) alkaline and (D) subcritical water extracts.

from longer stretches of X2U motifs in polymeric form of GX. SEC analysis also revealed a small difference in mass distribution after double digestion compared to single digestion with either GH10 or GH11 β-xylanase, which again points out to the occurrence of blockwise X_2U stretches in the xylan polymer structure.

Since X_2U represents the highly substituted xylan motifs in aspen GX, we compared xylan substitution pattern between digested and undigested fraction after GH30 enzyme treatment as revealed by 2D HSQC NMR (Supplementary Material Fig. S3). The undigested part is the fraction retained on the filter, while the digested (oligomeric) part passes through. The assignment of the main $^{13}C—^{1}H$ HSQC correlation signals are presented in the Supplementary Table S3. The spectra revealed that the main cross-peaks are from the xylose and the glucuronic acid substitution. The undigested sample had $^{13}C—^{1}H$ cross-peaks at 63.0,3.65/3.57 ppm, which match with previously reported carbon and proton shifts of a xylanase impurity (Bryant et al., 2020). The degree of substitution was estimated from the relative integrals on the anomeric region, as a ratio of the C1/H1 of the glucuronic acid to the C1/H1 of xylan (both X1 and XG1). This suggests that the digested xylan fraction has higher degree of glucuronidation compared to the undigested part, with 0.16 and 0.11, respectively. The higher degree of mGlcA substitution in the digested fraction suggests that the highly substituted X_2U blocks can be released into digested fraction by GH30. On the other hand, the lower degree of mGlcA substitution of the undigested part could be explained by enhanced aggregation and consequently lower accessibility for digestion by the GH30.

Evenly-spaced mGlcA substitutions, which are a pre-requisite for the twofold helical screw conformation of xylan major domain, have been proposed to be important for interaction of xylan with the hydrophilic surfaces of cellulose (Busse-Wicher et al., 2014; Grantham et al., 2017). On the other hand, the motifs with odd glucuronidation (for example, X_3U) are suggested to be part of the minor domains with three-fold helical screw conformation (Bromley et al., 2013; Martínez-Abad, Giummarella, Lawoko, Vilaplana, 2018). The occurrence of blockwise X_2U motifs in the aspen GX backbone in a 2-fold conformation suggests its dual potential; on one hand, the unsubstituted part of the screw can interact with the hydrophilic cellulose surfaces, whereas the opposite face of the 2-fold screw containing the mGlcA substitutions can provide specific microenvironments with acidic conditions pointing out of the cellulose surfaces, which could facilitate the connectivity with lignin though ester bonds in LCCs.

3.4. Occurrence of consecutive glucuronidation in aspen GX

The OLIMP profile of aspen GX digested with GH11 and GH30 showed specific oligosaccharides with *m/z* 1180 and *m/z* 1048, which putatively could correspond to a xylopentaose (X_5mU_2) and a xylotetraose with two mGlcA units (X_4mU_2), respectively (Fig. 2). Further reducing end labelling with anthranilic acid (AA), single ion monitoring (SIM) and mass fragmentation by LC-ESI-MS/MS was used to sequence the structure of these oligosaccharides and reveal the specific position of the two mGlcA units. Interestingly, for *m/z* 1180 (X_5U_2) only one major peak was detected in the LC-ESI-MS SIM chromatogram (Fig. 4A), evidencing the occurrence of a very conserved oligosaccharide sequence. The corresponding fragmentation pattern of the parent ion at *m/z* 1180 displayed the series of Y ions at Y_1 (*m/z* 272), Y_2 (*m/z* 404), Y_3 (*m/z* 726), and Y_4 (*m/z* 1048), revealing the univocal position of the mGlcA at the −3 and − 4 positions from the reducing end (Fig. 4B) and confirming the occurrence of consecutive glucuronidation in aspen GX. Similarly, the SIM chromatogram of the *m/z* 1048 oligosaccharide (X_4mU_2) released by GH30 only showed one oligosaccharide as well, and the subsequent fragmentation also confirmed the consecutive placement of the mGlcA substitutions (Fig. S4).

The relative intensity of the oligosaccharide profiling revealed that there is a relatively small population (less than 1 %) of oligosaccharides with consecutive glucuronidation in aspen GX (Fig. 2C). Similarly, a low

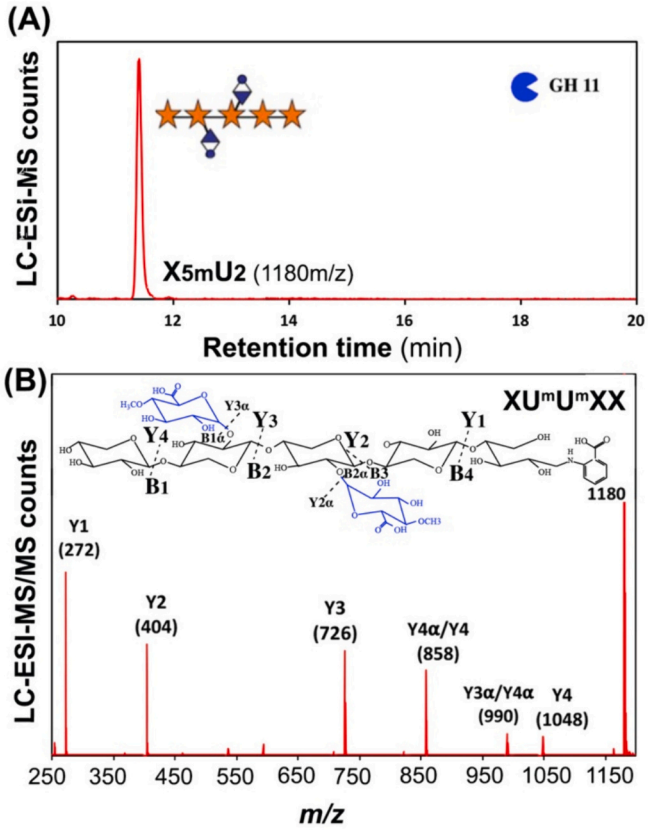

Fig. 4. Oligosaccharide sequencing of GX motifs with consecutive glucuronation. (A) Single ion monitoring (SIM) chromatogram of X5U2 oligomers released by GH11 glucuronoxylanase. (B) Oligosaccharide fragmentation of X5U2 oligomers by MS/MS. Assignation of the ion fragments according to the nomenclature proposed by (Domon & Costello, 1988). Note X = Xyl; U = mGlcA.

proportion of xylooligosaccharides with consecutive mGlcA decorations was reported in softwood AGX (Martínez-Abad et al., 2017). This low abundance of consecutively glucuronosylated xylan motifs could be explained by two possibilities; 1) low extractability due to their closer interaction with recalcitrant components like lignin or 2) relatively high cost of synthesizing this motif to plants. In softwoods, the low extractability of this GX motif population indicates their most likely tight interaction with lignin (Martínez-Abad, Jiménez-Quero, & Wohlert, 2020). Similarly, in the present study, the relative intensity of the signals corresponding to oligosaccharides with consecutive glucuronidation increased with longer extraction time, supporting the hypothesis of their increased recalcitrance.

Glucuronidation spacing pattern is a unique characteristic that differentiates xylans from softwood and hardwood species. So far, the occurrence of consecutive glucuronidation has only been reported for softwood AGX, where the presence of mGlcA was identified on adjacent xylose units as part of a minor domain (Martínez-Abad et al., 2017; Martínez-Abad, Jiménez-Quero, & Wohlert, 2020). Here we demonstrate that consecutive glucuronation can be found as well in hardwood xylans, which directly points out to a very specific regulation during xylan biosynthesis. In conifers, the study of the glucuronyl spacing pattern by the GUX (GlucUronic acid substitution of Xylan) genes indicates the presence of two distinct clades of GUX that independently regulate the even and consecutive mGlcA branching patterns in AGX. Clade 1 is responsible for most predominant spacing pattern of one GlcA in every 6 xylose units, while clade 2 could be responsible for the glucuronidation on consecutive xylose units (Lyczakowski et al., 2021). The conifer GUX clade 2 showed a high similarity with hardwood GUX2/4/5

(Lyczakowski et al., 2021), suggesting that this clade might be responsible for the here reported consecutive glucuronidation in aspen GX.

3.5. Even and consecutive spacing of O-acetyl substituents in aspen GX

The OLIMP of the GH30 released oligomers from GX extracted by SWE revealed the acetyl substitution pattern and their relative abundance (Fig. 2 E,F). The occurrence of a tight spacing pattern of acetylation in aspen GX was evident from the relatively high abundance of short acetylated UXOs, such as X2mUAc (one acetyl in every 2 xylose units) and X_3mUAc_{1-2} (with 1–2 acetyl in every 3 xylose). Moreover, the most abundant UXOs such as X_4mUAc_n and X_5mUAc_n displayed varied number of acetylations (between $n = 1$–4 acetylations), which should correspond with different putative acetylation patterns.

Reducing end labelling of the oligosaccharides followed by LC-ESI-MS/MS analysis was used to locate the position of acetyl substitutions within the linear and glucuronidated xylo-oligosaccharides released from aspen GX by xylanolytic enzymes. As an example, Fig. 5A shows the single ion monitoring (SIM) chromatograms for the series of acetylated X_5mUAc_n released by GH30 hydrolysis of aspen GX. Interestingly, X_5mUAc (*m/z* 1032) and X_5mUAc_3 (*m/z* 1116) showed mainly the occurrence of one large peak for each series (peaks (1) and (8), respectively), together with other minor peaks corresponding to other isomers (peaks (6) and (7) for X_5mUAc_3 at *m/z* 1116). On the contrary, the oligosaccharides corresponding with X_5mUAc_2 (*m/z* 1074) showed the occurrence of 4 peaks (peaks (2), (3), (4) and (5) corresponding with different isomeric oligosaccharides that differ in the position of the acetyl groups. ESI-MS/MS fragmentation of peak (1) revealed the position of the acetyl group in the same Xyl*p* unit bearing the mGlcA substitution corresponding to a $XXXXU^{4m2+3a}X$ structure (Fig. S5), in agreement with previous observations for birch and *Arabidopsis* (Busse-Wicher et al., 2014; Martínez-Abad, Giummarella, Lawoko, Vilaplana, 2018). For X_5mUAc_3, the most predominant peak (8) showed an evenly-spaced position of the Ac groups in the Xyl units at both the −2 and − 4 positions ($XX^{2a+3a}XU^{4m2+3a}X$) in the backbone (Fig. 5B), suggesting an extremely controlled placement of the acetyl substituents in the acetylated UXOs (Busse-Wicher et al., 2014; Martínez-Abad, Giummarella, Lawoko, Vilaplana, 2018). The occurrence of such controlled even pattern of acetylation has been shown to be critical for the prevalence of xylan interactions with cellulose surfaces in a flat 2-fold screw (Grantham et al., 2017), and here appears as the main motif in the acetylated xylo-oligosaccharides. However, ESI-MS/MS sequencing of the minor peaks (6) and (7) revealed the occurrence of other acetylation motifs in aspen GX. The peak (6) displayed a consecutive pattern of acetylation at −2, −3 and − 4 positions ($XX^{2a/3a}X^{2a/3a}XU^{4m2+3a}X$), whereas peak (7) showed a consecutive acetyl spacing at −2 and − 3 positions ($XXX^{2a+3a}U^{4m2+3a}X$). Finally, the ESI-MS/MS fragmentation of the oligosaccharide isomers corresponding with X5mUAc2 (*m/z* 1074) enabled the sequencing of acetylated oligosaccharide structures corresponding both even ($XXX^{2a/3a}XU^{4m2+3a}X$) and consecutive ($XXXX^{2a/3a}U^{4m2+3a}X$)) acetylation (Fig. S6). It is worth mentioning that from the ESI-MS/MS fragmentation of the acetylated oligosaccharides it is not possible to distinguish the regioselectivity of the acetylated units, this is, whether they are *O*-2 or *O*-3 acetylated.

The occurrence of consecutive acetylation was also evident from the elucidation of the acetyl position through the ESI-MS/MS fragmentation of linear acetylated xylo-oligosaccharides released by GH30 (Fig. S7) and GH10 and GH11 enzymes (Fig. S8). Such consecutive pattern of acetylation has been previously reported as well in GX extracted from Arabidopsis stems (Chong et al., 2014); however, to our best knowledge this consecutiove acetylation pattern has not been previously reported in hardwood xylans. Our results confirm that the acetylation of the hemicelluloses from hardwood trees is more complex than previously proposed and can occur on alternate and consecutive xylose units, as reported for softwood galactoglucomannans (Martínez-Abad, Jiménez-Quero, & Wohlert, 2020).

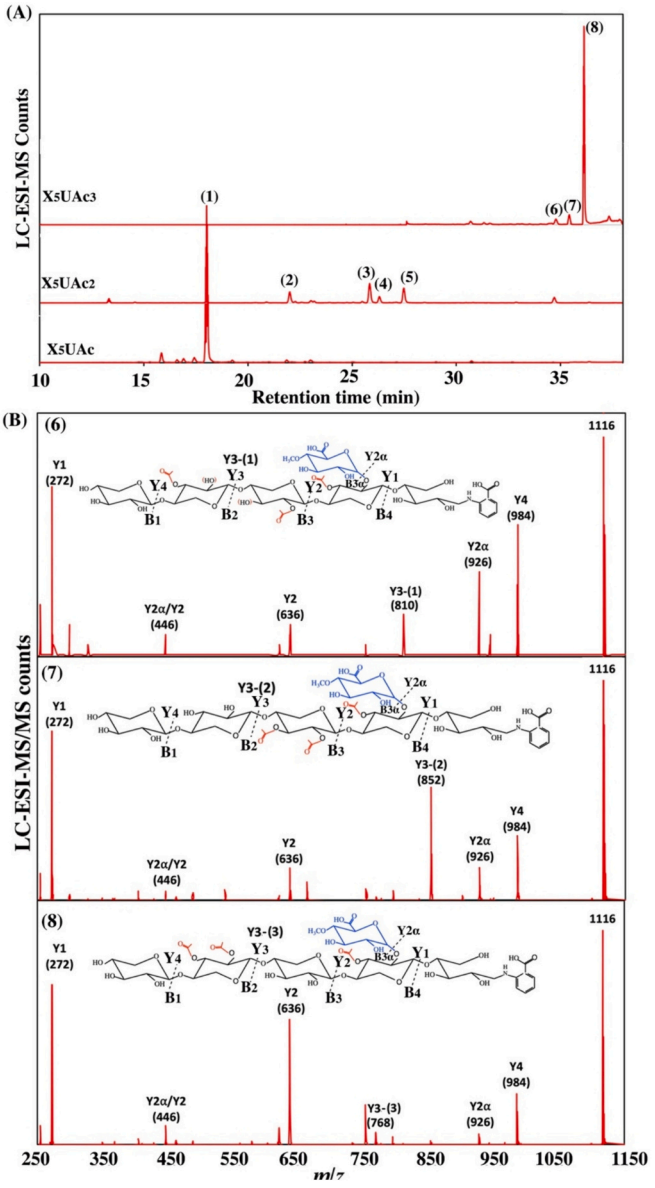

Fig. 5. Oligosaccharide sequencing of acetylated GX extracted using subcritical water from aspen wood. A. Single ion monitoring (SIM) chromatograms of the X_5UAc_n isomers released by GH30 glucuronoxylanase corresponding to X_5mUAc (m/z 1032), X_5mUAc_2 (m/z 1074) and X_5mUAc_3 (m/z 1116). B. Fragmentation of selected peaks corresponding to X_5mUAc_3 (m/z 1116) isomers by MS/MS and assignment of the ion fragments according to the nomenclature proposed by Domon & Costello, 1988. X = Xyl; mU = mGlcA; Ac = Acetyl.

O-acetyl substitutions are the most abundant decoration of xylan and play an important role in the plant cell wall physiology. The presence of *O*-acetyl substituents in xyloglucans and xylans was demonstrated to hinder the enzymatic breakdown of the polymer (Biely & Mackenzie, 1986; Gille et al., 2011). Interestingly, both uronilated and linear xylo-oligosaccharides produced by GH10, GH11 and GH30 family enzymes revealed the absence of acetyl substitutions in the −1 subsite (reducing end) position, suggesting that none of these enzymes exhibit catalytic activity when an acetyl group is present in the structure. Our results are thus in agreement with previous reports that the presence of acetyl groups provides resistance to cleavage by β-xylanases by blocking the access to the −1 position of their active site (Biely et al., 2004). Moreover, acetyl substitutions in the xylan backbone are suggested to prevent the xylan from precipitating and to provide a hydrophobic surface for

interaction with lignin (Busse-Wicher, Grantham, et al., 2016; Grantham et al., 2017; Pawar et al., 2013). The even pattern of acetylation in major domains is fundamental to maintain the xylan conformation as a twofold helical screw, which facilitates the interaction of the unsubstituted face of xylan with the hydrophilic cellulose surfaces and prevents cellulose crystallites from aggregating (Busse-Wicher et al., 2014). On the other hand, the consecutive acetylation pattern in minor domains might favor the occurrence of flexible threefold conformations in xylan with higher hydrophobic nature, which might promote interactions with the hydrophobic lignin matrix.

3.6. Proposed model of the role of xylan intramolecular motifs on the supramolecular architecture of aspen cell wall

In this work we have thoroughly studied the molecular structure of acetylated glucuronoxylan extracted from aspen wood under alkaline and subcritical water conditions using mass spectrometric approaches. The use of specific xylanolytic enzymes for the selective deconstruction of the xylan structure into amenable oligosaccharides for sequencing has revealed a much more complex and controlled palette of intramolecular motifs in terms of glucuronation and acetylation than previously reported (Fig. 6A). Acetylated GX from aspen shows an abundant domain with even glucuronation and acetylation, in agreement with has been previously reported for other hardwood species such as *Arabidopsis* and birch (Bromley et al., 2013; Busse-Wicher et al., 2014; Chong et al., 2014; Martínez-Abad, Giummarella, Lawoko and Vilaplana, 2018). This even placement of acetyl and glucuronyl decorations is critical for the interaction of xylans with cellulose surfaces in a rigid twofold conformation (Grantham et al., 2017; Simmons et al., 2016), as it enables the decorations to be placed facing off the cellulose surfaces (Fig. 6B). Interestingly, we have identified a higher abundance of tight and even $X_2U(Ac)$ motifs in aspen xylan, which seem to appear blockwise within the intramolecular sequence. The occurrence of such even $X_2U(Ac)$ blocks will be able on one hand to interact closely with cellulose surfaces, and on the other hand, will provide microenvironments with acidic conditions due to the close proximity of glucuronic acid motifs (Fig. 6B). The function of such acidic microenvironments is still unknown but they could be involved in modulating the hydrated pH environment within the plant cell wall or could be involved in the catalytic coupling with lignin through ester linkages in lignin-carbohydrate complexes (Giummarella & Lawoko, 2016; Takahashi & Koshijima, 1988).

On the other hand, we have identified as well the presence of domains with odd glucuronation spacing (mainly X_5mUAc_n) but with preserved even acetylation pattern. Interestingly, we have identified the occurrence of minor intramolecular domains with consecutive placement of glucuronic acid and acetyl substitutions. The occurrence of consecutive acetylation has been reported before for *Arabidopsis* (Chong et al., 2014), and may have a role in increasing the flexibility of the xylan chain (Berglund et al., 2020), serve as signaling motifs in the plant innate protection machinery (Escudero et al., 2017), and/or provide specific microenvironments with increased hydrophobicity, which could favor interactions with lignin moieties in the plant cell wall (Giummarella & Lawoko, 2016; Martínez-Abad, Giummarella, Lawoko and Vilaplana, 2018). Finally, we have reported for the first time the occurrence of consecutive glucuronation for hardwood xylan, in a similar manner that we previously identified for softwood xylans (Martínez-Abad et al., 2017). Such consecutive glucuronation motifs seem to be enriched in xylan fractions more recalcitrant to extraction (Martínez-Abad, Jiménez-Quero, & Wohlert, 2020), thus suggesting a role in modulating the occurrence of covalent linkages with lignin through lignin-carbohydrate complexes (Giummarella & Lawoko, 2016; Takahashi & Koshijima, 1988).

It is still unclear, however, whether the different molecular motifs are present in the same xylan polymeric populations, or are part of distinct individual xylan polymers within the aspen secondary cell wall. Unfortunately, the use of selective xylanolytic enzymes, required to obtain oligosaccharides amenable for mass spectrometry, prevents the study of the sequence of the intact xylan polymers. The separation of xylan polymers based on acidity and/or size has been so far unsuccessful, which supports a model where the different domains of glucuronation and acetylation are present in the same polymer (Bromley et al., 2013). However, recent studies on grass xylans by mutations of different glucosyltransferase enzymes responsible for introducing decorations on the xylan structure suggest the presence of different xylan polymeric populations with distinct intramolecular patterns of substitution (Tryfona et al., 2023; Tryfona et al., 2024). The question whether these different xylan polymers are present in different plant cell types or

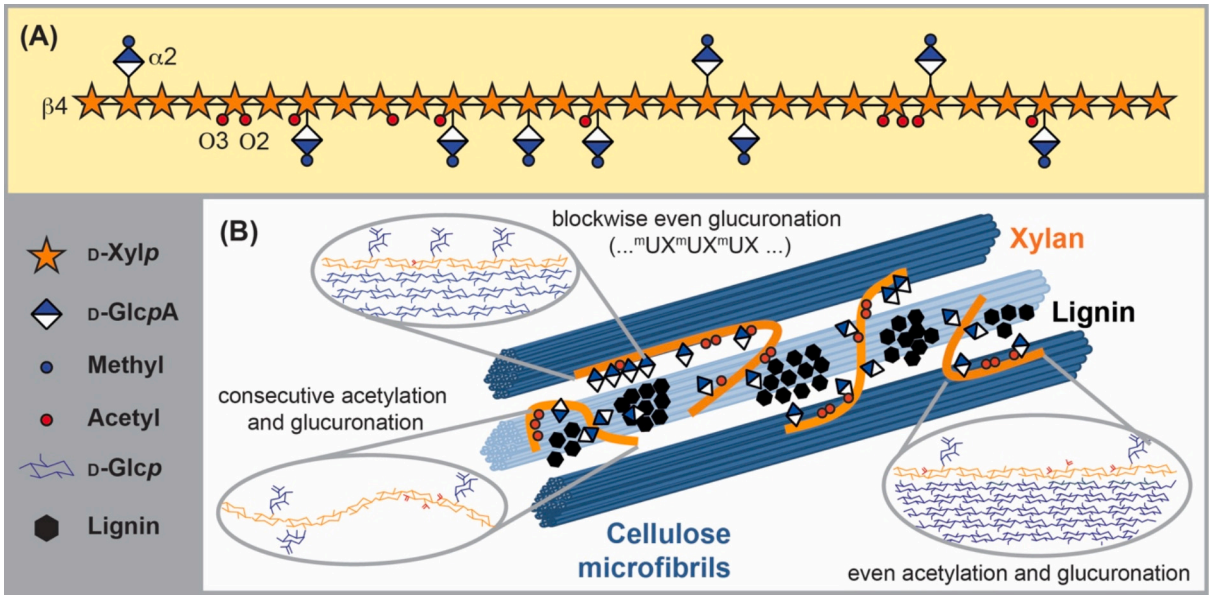

Fig. 6. (A) Diversity of molecular motifs in aspen glucuronoxylan, including the major domains with even pattern of glucuronation and acetylation, the specific blockwise X2U distribution of glucuronation, and the minor domains with consecutive glucuronation and acetylation. (B) Proposed model for the supramolecular organization of the xylan populations in aspen secondary cell wall. Aspen wood contains cellulose microfibrils of approximately 4 nm with 18 individual β-glucan chains. The xylan intramolecular motifs modulate the direct interactions with cellulose and lignin.

are universally distributed in the plant cell walls still remains fully unanswered (Boerjan et al., 2024).

4. Conclusions

In this study, we investigated the molecular structure of acetylated glucuronoxylan (GX) extracted from aspen with subcritical water and alkaline methods in terms of patterns of glucuronation and acetylation. ESI-LC-MS/MS analysis of oligomers generated by endoxylanases belonging to GH10, GH11 and GH30 families revealed the diversity of spacing of acetyl and 4-O-mGlcA substitutions in aspen GX. The main intramolecular domains corresponded with the previously reported even patterns of acetylation and glucuronation, which have been reported to be critical for rigid interactions with cellulose surfaces in a twofold conformation. Interestingly, a particular abundance of an even glucuronation spacing every two xylopyranose units was reported to occur blockwise (… $U^{4m2}XU^{4m2}XU^{4m2}X$ …), which might introduce acidic microenvironments on the surface of cellulosic fibres. Moreover, we have as well identified new intramolecular motifs distinct to those previously reported on other hardwood xylan species. We identified the occurrence of minor motifs with consecutive acetylation (acetyl group in adjacent xylose units) as opposed to the major domains with even acetylation spacing that has been mainly described for other hardwood trees. We also identified the occurrence of a unique feature corresponding with consecutive glucuronidation, which had only been described for softwood xylans before. This reveals that the intramolecular substitution pattern of acetylated xylans from hardwoods are far more complex than previously reported, and that there might be a possibility of phylogenetic evolution in the structural diversity of GX in both flowering plants and gymnosperms with common intramolecular patterns traditionally only described for species in one or other groups. Furthermore, these new insights into the diverse structural motifs in acetylated GX open new questions and possibilities to understand and modulate the molecular interactions of xylan with lignin and cellulose, which in turn contribute to the overall supramolecular architecture of plant woody tissues. Therefore, these findings have fundamental implications on developing hemicellulose-based strategies to overcome wood recalcitrance during biorefinery applications.

CRediT authorship contribution statement

Pramod Sivan: Writing – original draft, Methodology, Investigation, Formal analysis. **Emilia Heinonen:** Writing – review & editing, Methodology, Investigation. **Louis Escudero:** Methodology, Investigation, Formal analysis. **Madhavi Latha Gandla:** Methodology, Investigation, Formal analysis. **Amparo Jiménez Quero:** Writing – review & editing, Methodology, Investigation. **Leif J. Jönsson:** Writing – review & editing, Formal analysis. **Ewa J. Mellerowicz:** Writing – review & editing, Supervision, Formal analysis. **Francisco Vilaplana:** Writing – review & editing, Supervision, Resources, Project administration, Funding acquisition, Formal analysis, Conceptualization.

Declaration of competing interest

The authors declare the following financial interests/personal relationships which may be considered as potential competing interests: Francisco Vilaplana reports financial support was provided by Swedish Research Council. Francisco Vilaplana reports financial support was provided by European Union's Horizon 2020 research and innovation programme.

Data availability

Data will be made available on request.

Acknowledgements

The authors acknowledge the financial support from the Swedish Research Council (Project Grant 2020-04720) and the Knut and Alice Wallenberg Foundation (KAW) to the Wallenberg Wood Science Centre. F. V. and P. S. acknowledge the BioUPGRADE project for the financial contribution. BioUPGRADE has received funding from the European Union's Horizon 2020 research and innovation programme under grant agreement no. 964764. The content presented in this document represents the views of the authors, and the Commission is not responsible for any use that may be made of the information it contains. M. L. G. and L. J. J. acknowledge support from Bio4Energy (www.bio4energy.se). The authors are thankful for the access to the facilities and the technical assistance of the Biopolymer Analytical Platform, Umeå Plant Science Centre (UPSC), Umeå, for access to Pyrolysis-GC/MS analysis.

Appendix A. Supplementary data

Supplementary data to this article can be found online at https://doi.org/10.1016/j.carbpol.2024.122434.

References

Berglund, J., Kishani, S., Morais de Carvalho, D., Lawoko, M., Wohlert, J., Henriksson, G., … Vilaplana, F. (2020). Acetylation and sugar composition influence the (in)solubility of plant β-Mannans and their interaction with cellulose surfaces. *ACS Sustainable Chemistry & Engineering, 8*(27), 10027–10040.

Bi, R., Berglund, J., Vilaplana, F., McKee, L. S., & Henriksson, G. (2016). The degree of acetylation affects the microbial degradability of mannans. *Polymer Degradation and Stability, 133*, 36–46.

Biely, P., & Mackenzie, C. R. (1986). Cooperativity of esterases and xylanases in the enzymatic degradation of acetyl xylan. *Nature BioTechnology, 4*(8), 731–733.

Biely, P., Mastihubová, M., La Grange, D. C., Van Zyl, W. H., & Prior, B. A. (2004). Enzyme-coupled assay of acetylxylan esterases on monoacetylated 4-nitrophenyl β-D-xylopyranosides. *Analytical Biochemistry, 332*(1).

Boerjan, W., Burlat, V., Cosgrove, D. J., Dunand, C., Dupree, P., Haas, K. T., … Höfte, H. (2024). Top five unanswered questions in plant cell surface research. *The Cell Surface, 11*, Article 100121.

Bromley, J. R., Busse-Wicher, M., Tryfona, T., Mortimer, J. C., Zhang, Z., Brown, D. M., & Dupree, P. (2013). GUX1 and GUX2 glucuronyltransferases decorate distinct domains of glucuronoxylan with different substitution patterns. *Plant Journal, 74*(3), 423–434.

Bryant, N., Yoo, C. G., Pu, Y., & Ragauskas, A. J. (2020). 2D HSQC chemical shifts of impurities from biomass pretreatment. *ChemistrySelect, 5*(11).

Burton, R. A., Gidley, M. J., & Fincher, G. B. (2010). Heterogeneity in the chemistry, structure and function of plant cell walls. *Nature Chemical Biology, 6*, 724–732.

Busse-Wicher, M., Gomes, T. C. F., Tryfona, T., Nikolovski, N., Stott, K., Grantham, N. J., … Dupree, P. (2014). The pattern of xylan acetylation suggests xylan may interact with cellulose microfibrils as a twofold helical screw in the secondary plant cell wall of *Arabidopsis thaliana*. *The Plant Journal, 79*(3), 492–506.

Busse-Wicher, M., Grantham, N. J., Lyczakowski, J. J., Nikolovski, N., & Dupree, P. (2016). Xylan decoration patterns and the plant secondary cell wall molecular architecture. *Biochemical Society Transactions, 44*.

Busse-Wicher, M., Li, A., Silveira, R. L., Pereira, C. S., Tryfona, T., Gomes, T. C. F., … Dupree, P. (2016). Evolution of xylan substitution patterns in gymnosperms and angiosperms: Implications for xylan interaction with cellulose. *Plant Physiology, 171*(4), 2418–2431.

Charnock, S. J., Spurway, T. D., Xie, H., Beylott, M. H., Virden, R., Warren, R. A. J., … Gilbert, H. J. (1999). The topology of the substrate binding clefts of glycosyl hydrolase family 10 xylanases are not conserved. *Journal of Biological Chemistry, 273*(48).

Chong, S.-L., Virkki, L., Maaheimo, H., Juvonen, M., Derba-Maceluch, M., Koutaniemi, S., … Tenkanen, M. (2014). O-acetylation of glucuronoxylan in *Arabidopsis thaliana* wild type and its change in xylan biosynthesis mutants. *Glycobiology, 24*(6), 494–506.

Domon, B., & Costello, C. E. (1988). A systematic nomenclature for carbohydrate fragmentations in FAB-MS/MS spectra of glycoconjugates. *Glycoconjugate Journal, 5*(4).

Donev, E. N., Derba-Maceluch, M., Yassin, Z., Gandla, M. L., Pramod, S., Heinonen, E., … Mellerowicz, E. J. (2023). Field testing of transgenic aspen from large greenhouse screening identifies unexpected winners. *Plant Biotechnology Journal, 21*(5), 1005–1021.

Escalante, A., Gonçalves, A., Bodin, A., Stepan, A., Sandström, C., Toriz, G., & Gatenholm, P. (2012). Flexible oxygen barrier films from spruce xylan. *Carbohydrate Polymers, 87*(4), 2381–2387.

Escudero, V., Jordá, L., Sopeña-Torres, S., Mélida, H., Miedes, E., Muñoz-Barrios, A., … Molina, A. (2017). Alteration of cell wall xylan acetylation triggers defense responses that counterbalance the immune deficiencies of plants impaired in the β-subunit of the heterotrimeric G-protein. *The Plant Journal, 92*(3), 386–399.

Gandla, M. L., Derba-Maceluch, M., Liu, X., Gerber, L., Master, E. R., Mellerowicz, E. J., & Jönsson, L. J. (2015). Expression of a fungal glucuronoyl esterase in populus: Effects on wood properties and saccharification efficiency. *Phytochemistry, 112*(1).

Gerber, L., Eliasson, M., Trygg, J., Moritz, T., & Sundberg, B. (2012). Multivariate curve resolution provides a high-throughput data processing pipeline for pyrolysis-gas chromatography/mass spectrometry. *Journal of Analytical and Applied Pyrolysis, 95*, 95–110.

Gille, S., de Souza, A., Xiong, G., Benz, M., Cheng, K., Schultink, A., … Pauly, M. (2011). O-acetylation of Arabidopsis hemicellulose xyloglucan requires AXY4 or AXY4L, proteins with a TBL an DUF231 domain. *Plant Cell, 23*(11).

Giummarella, N., & Lawoko, M. (2016). Structural Basis for the Formation and Regulation of Lignin–Xylan Bonds in Birch. *ACS Sustainable Chemistry & Engineering, 4*(10), 5319–5326.

Giummarella, N., Pu, Y., Ragauskas, A. J., & Lawoko, M. (2019). A critical review on the analysis of lignin carbohydrate bonds. *Green Chemistry, 21*(7), 1573–1595.

Grantham, N. J., Wurman-Rodrich, J., Terrett, O. M., Lyczakowski, J. J., Stott, K., Iuga, D., … Dupree, P. (2017). An even pattern of xylan substitution is critical for interaction with cellulose in plant cell walls. *Nature Plants, 3*(11).

Hurlbert, J. C., & Preston, J. F. (2001). Functional characterization of a novel xylanase from a corn strain of Erwinia chrysanthemi. *Journal of Bacteriology, 183*(6).

Lawoko, M., Henriksson, G., & Gellerstedt, G. (2005). Structural differences between the lignin-carbohydrate complexes present in wood and in chemical pulps. *Biomacromolecules, 6*(6), 3467–3473.

Lyczakowski, J. J., Yu, L., Terrett, O. M., Fleischmann, C., Temple, H., Thorlby, G., … Dupree, P. (2021). Two conifer GUX clades are responsible for distinct glucuronic acid patterns on xylan. *New Phytologist, 231*(5).

Martínez-Abad, A., Berglund, J., Toriz, G., Gatenholm, P., Henriksson, G., Lindström, M., … Vilaplana, F. (2017). Regular motifs in Xylan modulate molecular flexibility and interactions with cellulose surfaces. *Plant Physiology, 175*(4), 1579–1592.

Martínez-Abad, A., Giummarella, N., Lawoko, M., & Vilaplana, F. (2018). Differences in extractability under subcritical water reveal interconnected hemicellulose and lignin recalcitrance in birch hardwoods. *Green Chemistry, 20*(11), 2534–2546.

Martínez-Abad, A., Jiménez-Quero, A., & Wohlert, J. (2020). Influence of the molecular motifs of mannan and xylan populations on their recalcitrance and organization in spruce softwoods. *Green Chemistry, 22*(12), 3956–3970.

McKee, L. S., Sunner, H., Anasontzis, G. E., Toriz, G., Gatenholm, P., Bulone, V., … Olsson, L. (2016). A GH115 α-glucuronidase from Schizophyllum commune contributes to the synergistic enzymatic deconstruction of softwood glucuronoarabinoxylan. *Biotechnology for Biofuels, 9*(1).

Mikkelsen, D., Flanagan, B. M., Wilson, S. M., Bacic, A., & Gidley, M. J. (2015). Interactions of Arabinoxylan and (1,3)(1,4)-β-glucan with cellulose networks. *Biomacromolecules, 16*(4), 1232–1239.

Mischnick, P. (2012). Mass spectrometric characterization of oligo- and polysaccharides and their derivatives. *Advances in Polymer Science, 248*.

Nieduszynski, I., & Marchessault, R. H. (1971). Structure of β-D-(1→4′)Xylan hydrate. *Nature, 232*, 46–47.

Pawar, P. M. A., Koutaniemi, S., Tenkanen, M., & Mellerowicz, E. J. (2013). Acetylation of woody lignocellulose: Significance and regulation. *Frontiers. Plant Science, 4*.

Pell, G., Szabo, L., Charnock, S. J., Xie, H., Gloster, T. M., Davies, G. J., & Gilbert, H. J. (2004). Structural and biochemical analysis of Cellvibrio japonicus xylanase 10C: How variation in substrate-binding cleft influences the catalytic profile of family GH-10 xylanases. *Journal of Biological Chemistry, 279*(12).

Pollet, A., Delcour, J. A., & Courtin, C. M. (2010). Structural determinants of the substrate specificities of xylanases from different glycoside hydrolase families. *Critical Reviews in Biotechnology, 30*.

Santos, R. B., Lee, J. M., Jameel, H., Chang, H. M., & Lucia, L. A. (2012). Effects of hardwood structural and chemical characteristics on enzymatic hydrolysis for biofuel production. *Bioresource Technology, 110*, 232–238.

Simmons, T. J., Mortimer, J. C., Bernardinelli, O. D., Pöppler, A.-C., Brown, S. P., deAzevedo, E. R., … Dupree, P. (2016). Folding of xylan onto cellulose fibrils in plant cell walls revealed by solid-state NMR. *Nature Communications, 7*, 13902.

Sivan, P., Heinonen, E., Latha Gandla, M., Jiménez-Quero, A., Özeren, H. D., Jönsson, L. J., … Vilaplana, F. (2023). Sequential extraction of hemicelluloses by subcritical water improves saccharification of hybrid aspen wood grown in greenhouse and field conditions. *Green Chemistry, 25*(14), 5634–5646.

Smith, P. J., Wang, H. T., York, W. S., Peña, M. J., & Urbanowicz, B. R. (2017). Designer biomass for next-generation biorefineries: Leveraging recent insights into xylan structure and biosynthesis. *Biotechnology for Biofuels, 10*.

St John, F. J., Hurlbert, J. C., Rice, J. D., Preston, J. F., & Pozharski, E. (2011). Ligand bound structures of a glycosyl hydrolase family 30 glucuronoxylan xylanohydrolase. *Journal of Molecular Biology, 407*(1).

Takahashi, N., & Koshijima, T. (1988). Ester linkages between lignin and glucuronoxylan in a lignin-carbohydrate complex from beech (Fagus crenata) wood. *Wood Science and Technology, 22*(3), 231–241.

Timell, T. E. (1961). Isolation of galactoglucomannans from the wood of gymnosperms. *Tappi, 44*(2).

Tryfona, T., Bourdon, M., Delgado Marques, R., Busse-Wicher, M., Vilaplana, F., Stott, K., & Dupree, P. (2023). Grass xylan structural variation suggests functional specialization and distinctive interaction with cellulose and lignin. *The Plant Journal, 113*(5), 1004–1020.

Tryfona, T., Pankratova, Y., Petrik, D., Rebaque Moran, D., Wightman, R., Yu, X., … Dupree, P. (2024). Altering the substitution and cross-linking of glucuronoarabinoxylans affects cell wall architecture in Brachypodium distachyon. *New Phytologist, 242*(2), 524–543.

Urbániková, Ā., Vršanská, M., Mārkeberg Krogh, K. B. R., Hoff, T., & Biely, P. (2011). Structural basis for substrate recognition by Erwinia chrysanthemi GH30 glucuronoxylanase. *FEBS Journal, 278*(12).

Willför, S., Sundberg, A., Pranovich, A., & Holmbom, B. (2005). Polysaccharides in some industrially important hardwood species. *Wood Science and Technology, 39*, 601–617.

Yu, Z., Gwak, K. S., Treasure, T., Jameel, H., Chang, H. M., & Park, S. (2014). Effect of lignin chemistry on the enzymatic hydrolysis of woody biomass. *ChemSusChem, 7*(7), 1942–1950.